CEBAF Program Advisory Committee Six (PAC6) Proposal Cover Sheet

This proposal must be received by close of business on April 5, 1993 at:

CEBAF
User Liaison Office
12000 Jefferson Avenue
Newport News, VA 23606

Proposal Title

"The Δ(1232) Form Factor at High Momentum Transfers"

Contact Person

Name: Paul Stoler
Institution: RPI
Address: Physics Dept.,
Address: Rensselaer Polytechnic Institute
City, State ZIP/Country: Troy, NY 12180
Phone: (518) 276-8388 **FAX:** (518) 276-8860
E-Mail → BITnet: STOLER@RPITSMTS **Internet:** STOLERP@RPIMEP.PHYS.RPI.EDU

If this proposal is based on a previously submitted proposal or letter-of-intent, give the number, title and date:

CEBAF Use Only

Receipt Date: 4/5/93 Log Number Assigned: PR 93-035

By: gp

Proposal for the

CEBAF Program Advisory Committee

The $\Delta(1232)$ Form Factor at High Momentum Transfer

P. Stoler (co-spokesperson), J. Napolitano (co-spokesperson), G. Adams, B. Wojtsekhowski, N. Mukhopadhyay (theory)

PhysicsDept., Rensselaer Polytechnic Inst., Troy, NY 12180

R. Carlini, Y. Chen, D. Mack, J. Mitchell and S. Wood

CEBAF, 12000 *JeffersonAve., NewportNews, VA*23606

E. Kinney, R.J. Peterson, R. Ristinen

PhysicsDept., Univ. of Colorado, Boulder, CO 80309

Abstract: We propose to measure the transition amplitudes of the $\Delta(1232)$ resonance at $Q^2 = 4\ GeV^2/c^2$. In particular we will measure the kinematically complete reaction $p(e,e'p)\pi^\circ$ at excitation energies covering the $\Delta(1232)$, obtaining nearly a full 4π angular distribution of the $p-\pi^\circ$ in the Δ rest frame. The experiment will be carried out in Hall-C using the Short Orbit Spectrometer (SOS) to detect the scattered electrons, and the High Momentum Spectrometer (HMS) to detect the proton. At these cm energies only single meson production is kinematically allowed. However the π° will be definitely identified by missing mass reconstruction. We will obtain information about the transition multipole amplitudes for this reaction in a kinematic region never previously accessed. An important goal will be to assess the relative importance of the contributing amplitudes M_{1+} , E_{1+} and S_{1+}. At low Q^2 in the region where the constituent quark model works well, the M_{1+} amplitude dominates and the E_{1+} and S_{1+} are small. At increasing Q^2 there is no reason to expect E_{1+} to remain small. Indeed, an increasing E_{1+} would be the signature of the breakdown of the constituent quark model as a basis for describing the properties of baryons, and is fully expected by theoretical models.

The experiment is will utilize a 4 GeV, 100 μA beam, and 4 cm liquid hydrogen target. There will be one setting of the electron spectrometer which defines Q^2. In order to cover the 4π decay of the delta it will be necessary to have up to 4 angular settings of the proton spectrometer to cover the full range of proton momenta. The experiment will use only the initial complement of equipment in Hall C, with no further additions or modifications. Data collection time will be about 10 ***days*** (240 ***hrs***). The total request including contingency is 300 ***hrs***.

I. Proposal Summary

This experiment will measure exclusive single π° production on protons in the excitation region of the $\Delta(1232)$ resonance at $Q^2 = 4\ GeV^2/c^2$. The experiment will be carried out in Hall-C using the Short Orbit Spectrometer (SOS) to detect the scattered electrons, and the High Momentum Spectrometer (HMS) to detect the recoiling proton. The emitted pions will be identified by missing mass reconstruction. We will study the short range structure of the Δ resonance in a kinematic region which has never before been studied by exclusive coincidence reactions. A specific goal is to identify the transition from the $non-perturbative\ QCD$ regime , where theoretical descriptions have used constituent quark models (CQM), toward a physical region where CQM no longer apply, and different degrees of freedom are necessary to describe the experimental results. There is evidence that for baryons this transition already may be occurring at $Q^2 \sim 2$ or 3 GeV^2/c^2, which is comfortably below the Q^2 of this proposal. A unique feature of the $\Delta(1232)$ which we would like to understand is the decrease in the form factor as a function of Q^2 relative to the other known resonances, both in the low Q^2 $non-perturbative$ region as well as in the transition region where different physics is likely to play a role.

A specific signature for the breakdown of the CQM is the evolution of the contributing amplitudes from those predicted by CQM's. In particular the existence of a sizeable E_{1+} amplitude is one such signature. As will be seen in Section IV, the ability to observe

this reaction over the full 4π resonance decay solid angle in the center-of-mass, makes this experiment very sensitive to the admixture of the contributing multipoles.

The objective of this experiment is to measure the decay angular distribution of the Δ at the highest Q^2 possible with a 4 GeV beam and existing apparatus. At $Q^2 = 4$ GeV^2/c^2 there is a good match to the characteristics of the HMS and SOS spectrometers. This gives us the opportunity to obtain a definitive signature of the onset of the transition from CQM toward a $PQCD$ description at a very early stage in CEBAF's operation.

II. Physics Background

One of the fundamental problems in physics concerns the structure of hadrons (mesons and baryons) and their excitations in terms of quark and gluon constituents. A central question concerns which models are valid for describing these excitations in different domains of Q^2. At low Q^2 (< 1 GeV^2/c^2) in the *non − perturbative* QCD ($NPQCD$) domain, CQM have been used to describe available data - sparse as they are. In the limit of very high Q^2 it is widely believed that *perturbative* QCD ($PQCD$) descriptions would be appropriate. However, there is currently strong disagreement as to what domain of Q^2 corresponds to the transition from $NPQCD$ to $PQCD$ descriptions. Some (Br-89, Ca-88, Li-92) believe the transition may take place for Q^2 as low as a few GeV^2/c^2 while others maintain that the transition should occur in a much higher region of Q^2 (Is-89, Ra-91). Recently, calculations taking into account color radiative (*Sudakov*) effects (Li-92) support the former point of view.

During the past several years, proton elastic scattering form-factor data (Ar-86, Am-92) have provided some of the primary data for testing these questions. This data provides strong evidence that CQM's cannot be applied for $Q^2 >$ a few GeV^2/c^2. For example Figure 1 shows the result of a relativistically invariant CQM calculation of the proton magnetic form factor (Dz-88) compared with the experimental data. Already at $Q^2 = 2$ - 3 GeV^2/c^2 the theory significantly underestimates the experimental results. Though the calculation utilized a Gaussian potential, which introduces large damping, the underestimation of the form factor at high enough Q^2 would occur for any CQM with a confining potential.

The study of the properties of electromagnetic transitions to resonant excited states is also a very important area for testing models of baryon structure. This is reviewed in St-93. Unfortunately not much is known for Q^2 greater than a few GeV^2/c^2. This is because the resonances are broad, strongly overlapping, with a significant underlay of non-resonant background. This is seen in single arm data of Figure 2. Although one observes three peaks, there are some 20 known light-quark resonances of mass less than 2 GeV.

Transition Multipoles

The way to get at the multipoles of the individual resonances is to perform coincidence

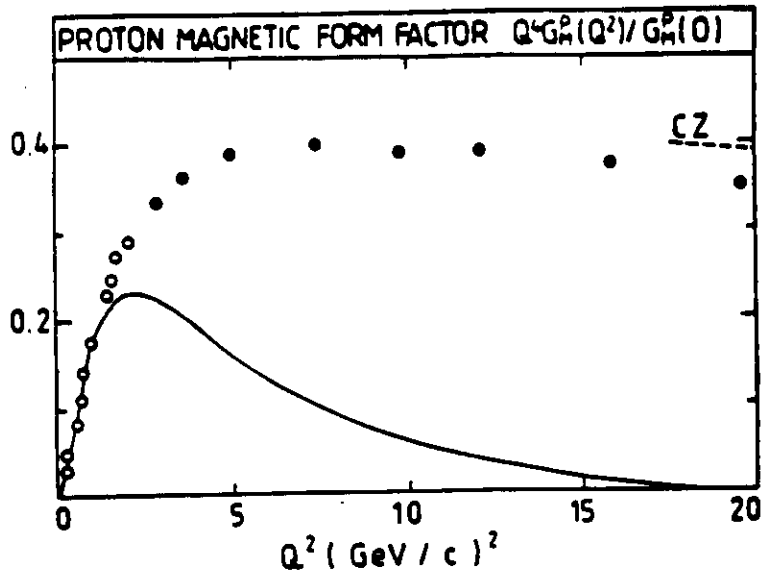

Figure 1. The proton elastic magnetic form factor G_M calculated by Da-88, compared to the experimental data of Ar-86.

experiments in which the angular dependences of the decay products are analyzed. In this regard the $\Delta(1232)$ is the most favorable case to study, since as seen in Figure 2, it is the only resonance which does not strongly overlap any of the others. Furthermore, its only strong decay is by single pion emission, and the level of underlying background can be strongly reduced by selecting the π° channel, since the normally dominant *seagull* and $t-$ *channel* background terms are absent. From the physics point of view the $\Delta(1232)$ has the additionally attractive feature that $J = 3/2$, so that there are three contributing multipoles, E_{1+}, M_{1+}, and S_{1+} whose relative contributions are model dependent.

At low Q^2 in a pure $SU(6)$ *non – relativistic* CQM the $N \rightarrow \Delta$ transition is purely M_{1+} in character, involving a single-quark spin-flip with $\Delta L = 0$. An E_{1+} contribution is not permitted since the Δ and N are both in $L = 0$ states which cannot be connected by an operator involving $L > 0$. The addition of a residual quark-quark color magnetic interaction adds higher L components to the Δ wave function, and thus introduces a small E_{1+} component of perhaps a few percent. The measurement of this small E_{1+}/M_{1+} ratio is one of the most interesting problems in baryon resonance physics in that it will give very powerful tests of the CQM in the low Q^2 regime. At $Q^2 = 0$ the experimental data supports the CQM prediction of M_{1+} dominance extremely well.

A review by Da-90,91 finds

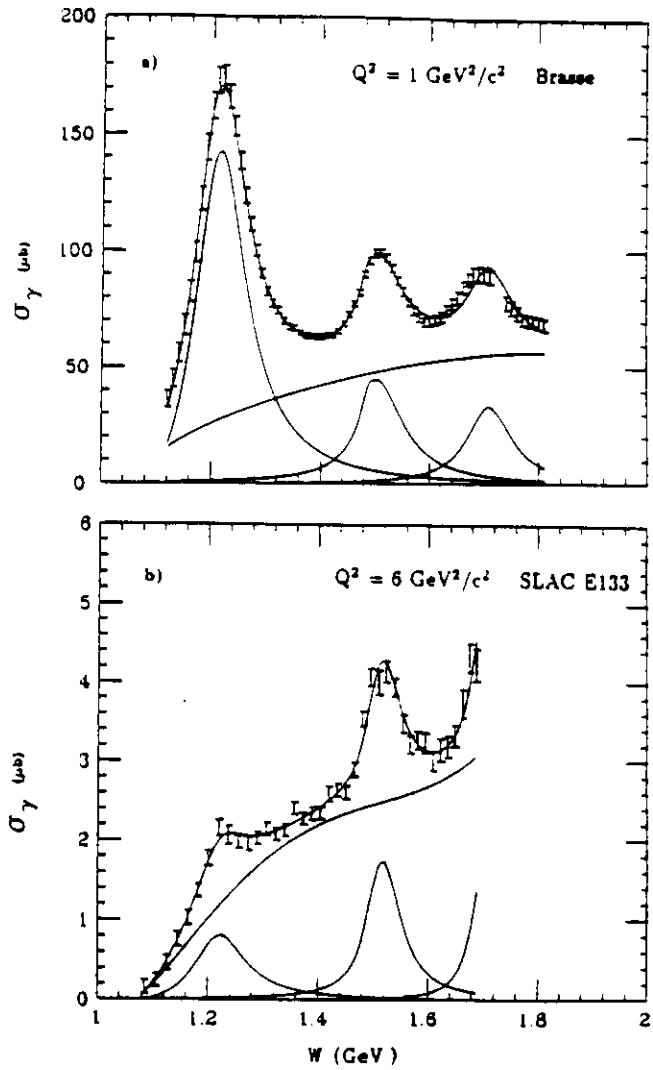

Figure 2. The virtual photon excitation curves for electron scattering at $Q^2 = 1$ and 6 GeV^2/c^2. Figure from St-91a.

$$M_{1+} = 285 \pm 37 \times 10^{-3}\ GeV^{-1}$$

$$E_{1+} = -4.6 \pm 2.6 \times 10^{-3}\ GeV^{-1}.$$

As Q^2 increases there is no reason to expect the E_{1+}/M_{1+} ratio to remain extremely small. For $Q^2 > 0$ the experimental situation is shown in Figure 3 as summarized by Bu-92.

Nearly all the available data is for $Q^2 < 1\ GeV^2/c^2$. The fact that $Re(E^*_{1+}M_{1+})/|M_{1+}|^2$ ($\equiv E/M$) remains very small is further evidence that the CQM continues to work well for low Q^2. The one experimental point at $Q^2 = 3\ GeV^2/c^2$ ($E/M = 0.8 \pm 0.6$) is statistically not significant enough to make any conclusions, although it is suggestive. In any case, this was extracted by fitting data under the assumption that E/M is very small so that various multipole contributions in the data are neglected. However, Wa-90 have pointed out that one can obtain an equally consistent fit to the data on which the analysis

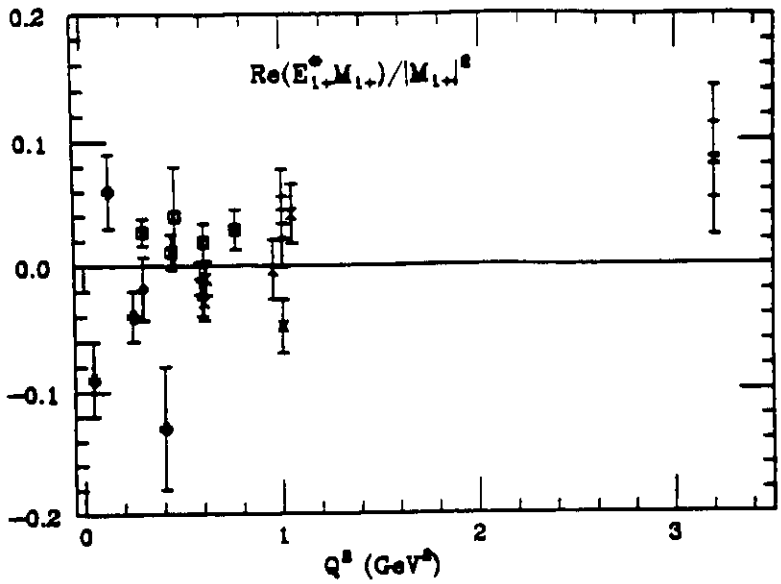

Figure 3. Evaluation of the $Re(E^*_{1+}M_{1+})/|M_{1+}|^2$ evaluated by Bu-92.

is based by assuming in fact that $E/M \sim 1$ so that we must conclude that the magnitude of E/M at $Q^2 = 3\ GeV^2/c^2$is unknown.

What does one expect above $Q^2 \sim 2\ GeV^2/c^2$? At this point, beyond the CQM based calculations there is no theoretical guidance. However, there is a theory which relates to high Q^2. It is believed that all exclusive reactions should proceed by leading order processes involving Fock states having the minimum number of current quarks (ie. the valence quark configuration) which exchange the minimum number of gluons. For a baryon, the transition amplitude is obtained by evaluation of diagrams such as shown in Figure 4.

Figure 4. Typical leading order diagram contributing to a baryon form factor at high Q^2.

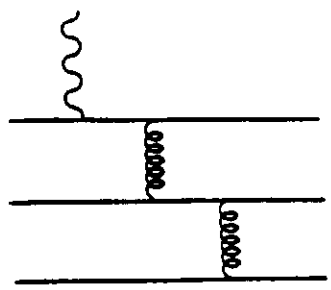

Such processes could in principle be evaluated perturbatively, since all momentum transfers between quarks and gluons are large.

A further constraint is that of *helicity conservation* at the vertices of the quarks with the vector fields, ie. photons and gluons. For electromagnetic processes involving

cylindrical symmetry this implies that the overall helicity of the baryon is conserved. Thus helicity non-conserving amplitudes are expected to vanish relative to helicity conserving amplitudes at the high Q^2 limit.

The multipoles may be expressed in terms of helicity conserving and non-conserving amplitudes as follows:

$$\Delta\lambda = 0 : A_{1+} = \tfrac{3}{2}M_{1+} + \tfrac{1}{2}E_{1+} \tag{1a}$$

$$\Delta\lambda = 2 : B_{1+} = E_{1+} - M_{1+} \tag{1b}$$

$$\Delta\lambda = 1 : C_{1+} = \frac{2Q^2}{p_\pi^*}S_{1+}. \tag{1c}$$

Thus, helicity conservation implies $B_{1+} = 0$, or $E_{1+} = M_{1+}$. This is quite different from the low Q^2 situation. In the present experimental situation, we do not expect to have reached the *perturbative* regime, however we do expect to observe a significant increase in E_{1+}/M_{1+}. Recently Li-92 has shown that color radiative corrections (*Sudakov* effects) reduce the non-leading contributions to elastic form-factors (which dominate the CQM approach) relative to the leading contributions (which dominate the $PQCD$ approach) so that the transition from CQM to $PQCD$ occurs at lower values of Q^2 than might otherwise be expected. One may speculate that this may be the underlying reason why so many exclusive reactions appear to obey the simple Q^2 counting rules at unexpectedly low values of Q^2.

Form Factors

The current experimental situation, summarized in Figure 3, is that there exists no exclusive data above 3 GeV^2/c^2, and the data at 3 GeV^2/c^2 are quite sparse. Existing single-arm inclusive electron scattering data have been evaluated (St-91a,b), and form-factors extracted for the peaks corresponding to the first, second and third resonance regions. Transverse resonance form-factors G_T are defined (Ca-88) in analogy with elastic scattering form-factors:

$$\frac{d\sigma}{d\Omega dE} = \Gamma\sigma(W_R) \tag{2}$$

$$\sigma(W_R) = \frac{8\pi\alpha Q^2 M_N}{W_R K_R} G_T^2. \tag{3}$$

where $\sigma(W_R)$ is the virtual photon cross section at the resonance energy W_R, K_R is the equivalent real photon energy at W_R, and the quantity Γ is the virtual photon flux factor (see Appendix).

The evaluation of the leading order transition amplitudes for exclusive processes using $PQCD$ leads to Q^2 scaling laws, which remarkably appear to be obeyed even at relatively

low Q^2. For example, evaluation of diagrams such as in Figure 4 leads to a Q^{-4} behavior for helicity conserving form factors, and a greater fall off with Q^2 for helicity non-conserving form factors, eg Q^{-6} for $\Delta L = 2$. There is also a logarithmic decrease due to the Q^2 dependence of the running coupling constant α_s, but this would be observable only over a large range of Q^2.

Transition form-factors G_T for the $\Delta(1232)$ and the peaks near W = 1535 and 1680 MeV, as a function of Q^2 were obtained by fitting Breit-Wigner resonance shapes together with phenomenological backgrounds to existing inclusive data, such as in Figure 1. These are shown in Figure 5 relative to a dipole shape $G(Q^2)_{dipole} = 3/(1 + Q^2/0.71)^2$. Included in Figure 5 is the proton elastic form-factor. Also shown at lower Q^2 are form-factors extracted from data obtained from exclusive $(e, e', p)\pi^\circ$ and $(e, e', p)\eta$ experiments (Ha-79, Fo-83, Bu-91).

In Figure 5 the ratio $G_M(Q^2)/G(Q^2)_{dipole}$ is plotted rather than $Q^4 G_M(Q^2)$ to better display the low Q^2 behavior. For high Q^2 the quantity $Q^4 G(Q^2)_{dipole} \rightarrow const.$ In fact the elastic form-factor G_M does appear to approach this behavior above $Q^2 \sim 5\ GeV^2/c^2$ out to the highest measured Q^2 ($\sim 35\ GeV^2/c^2$). This Q^2 behavior as well as the magnitude (see below) has been one of the key elements in support of the proponents of $PQCD$ at experimentally accessible values of Q^2. The second and third resonance transition form-factors also appear to approach the predicted Q^{-4} behavior, within quite large statistical errors.

The $\Delta(1232)$ form-factor decreases faster than Q^{-4} at all observed Q^2, that is at low Q^2 where CQM's are expected to work well, as well as at higher Q^2 where CQM are not appropriate. The reason for this anomalous behavior is not currently understood, however it has been suggested (Ca-88) that this may be due to the suppression of the leading order $PQCD$ amplitude, and the dominance of higher order amplitudes in regions of Q^2 where leading order contributions are already important in other form factors.

IV. Experimental considerations

Acceptances: It is proposed to measure the reaction $p(e, e'p)\pi^\circ$ using the SOS spectrometer to detect the scattered electrons and the HMS spectrometer to measure the recoil protons. Due to a large kinematic boost at this high Q^2 the hadrons are always emitted in a narrow forward cone about the momentum transfer direction. This is illustrated in Figure 6.

Thus one sees that by detecting the proton it is possible to measure a 4π cm angular distribution with a moderate solid angle spectrometer. Also shown in Figure 6 is the vertical acceptance of the HMS. However, the horizontal acceptance of the HMS is rather narrow so that 4 horizontal angular settings will be required to cover the full solid angle (Figure 7). Likewise, the the momentum acceptance of the HMS is not great enough to cover the full range of proton momenta at a given angular setting, two and three will be

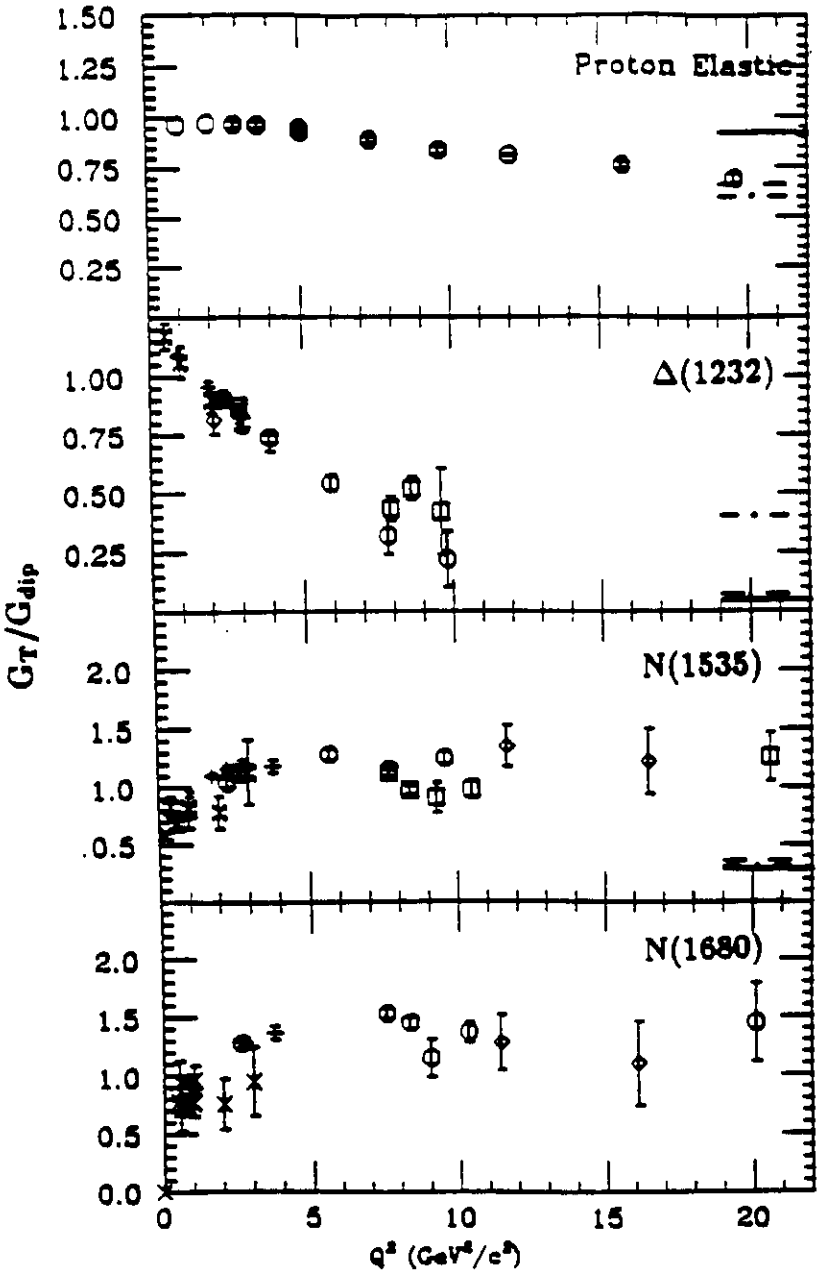

Figure 5. (a) The transverse magnetic form-factor divided by the dipole shape G_M/G_{dipole} verses Q^2 for elastic scattering from the proton. The data are from Ar-86. The curves at the right are the results of calculations (Ji-87) at $Q^2 = 20\ GeV^2/c^2$ using proton distribution functions C-Z (Ch-84), G-S (Ga-86), and K-S (Ki-87). (b - d) The analogous transverse form-factors G_T/G_{dipole} verses Q^2 obtained in St-91a,b for transitions to the first, second and third resonances respectively, where $G(Q^2)_{dipole} = 3/(1 + Q^2/0.71)^2$. The first resonance (b) is the $\Delta(1232)$. The second resonance (c) at lower Q^2 ($\sim 3\ GeV^2/c^2$) is mostly due to the $S_{12}(1535)$. The third resonance at low Q^2 is dominated by the $F_{15}(1680)$. The resonance form-factor G_T is defined in the text. The fits for G_T were based on available inclusive data reconstructed from data referred to in St-91a,b. Also shown at lower Q^2 denoted by (×) are form-factors derived from amplitudes obtained from exclusive $(e, e', p)\pi^0$ and $(e, e', p)\eta$ data, also referred to in St-91a,b. The errors shown are statistical. The curves on the right are the result of calculations by Ca-88 using the same proton distributions as in (a) with their derived baryon distribution functions.

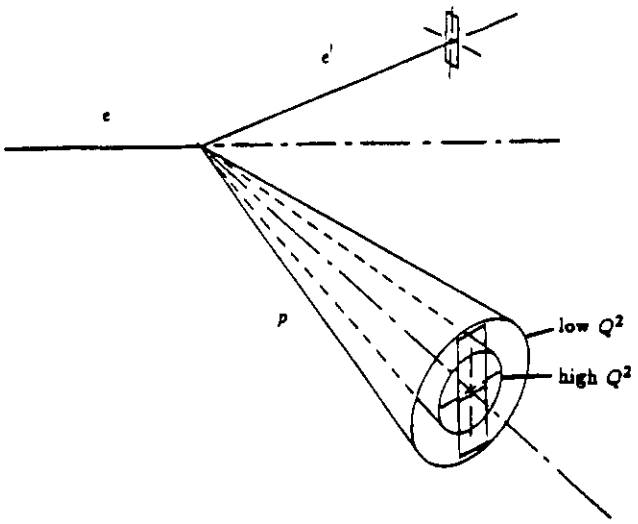

Figure 6. Illustration of the envelope of the proton laboratory angle relative to the momentum transfer vector.

necessary at each pair of angular settings. so that we estimate that we would require a total of about 10 angle-central momentum settings.

Figure 8 shows the cm decay angle and proton momentum coverage for each setting of the HMS spectrometer for an electron kinematics fixed at the center of the SOS acceptance. The finite acceptance of the SOS will broaden the acceptances shown in the figure.

Backgrounds: One of the major sources of background will be energetic pions misidentified as electrons. Most of these will be eliminated by the SOS gas Cerenkov counter. The remaining background will be eliminated using several techniques: coincidence timing, trajectory traceback to the target, and most importantly by by requiring the missing mass

$$(p_e + p_p - p_e' - p_p')^2 = m_\pi^2$$

The missing mass technique for π° and η electroproduction has been successfully used previously with magnetic spectrometers, eg. at DESY (Br-84). We will be in a more favorable situation than earlier work for several reasons. 1. We are working at an excitation energy where only one pion can be emitted, so that there will be no real multi-pion continuum. 2. The resolution of the SOS-HMS combination is much better than in other measurements, eg. Br-84, so that we will obtain a much narrower and higher π° peak.

V. Relationship Between Multipoles and Measured Data

With unpolarized beam and target the differential cross section as a function of pion

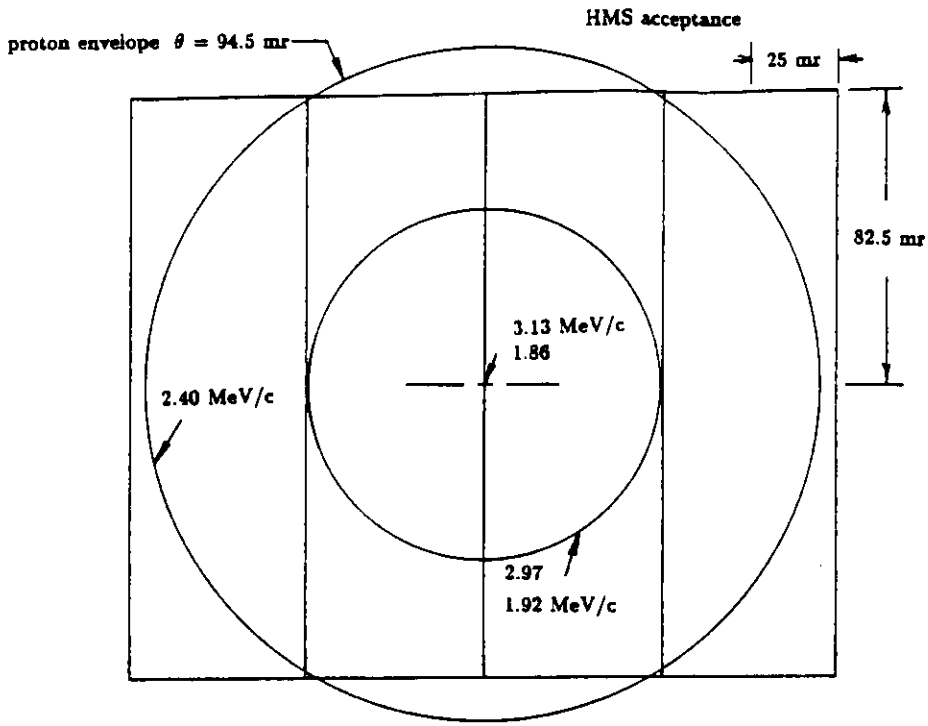

Figure 7. The acceptance of the HMS spectrometer for an electron kinematics fixed at the center of the SOS acceptance. The finite acceptance of the SOS will broaden the acceptances shown in the figure. The outer circle is the envelope of the maximum lab. angle of the cone corresponding to a full 4π cm decay.

angles (θ, ϕ) relative to the direction of the virtual photon may be expressed as

$$\frac{d\sigma}{d\Omega_\pi} = F\{A(\theta) + \epsilon B(\theta) + \epsilon C(\theta)cos(2\phi)sin^2\theta + \sqrt{\epsilon(\epsilon+1)}D(\theta)cos\phi sin\theta.\} \quad (4)$$

In the above

$$F \equiv \frac{|\vec{p}_\pi|W}{MK} \quad \text{with} \quad K = \frac{W^2 - M^2}{2M}. \quad (5)$$

In general, each resonance is characterized by three complex multipoles M_J, E_J and S_J. In the case of the $\Delta(1232)$ we have $J = l+1/2 \equiv l+$, with $l_+ = 1+$. In the region of the $\Delta(1232)$ the non resonant Born terms contribute significantly. However, the selection of the π° channel strongly suppresses the relative Born contributions in comparison with their contribution to the inclusive cross section. There are also relatively small contributions due to the tails of higher resonances which need to be included in the analysis of the measured cross sections.

In the this experiment the angular distribution will be very sensitive to the relative contributions of the E_{1+} and M_{1+} multipoles, even if $E_{1+} << M_{1+}$ (which in fact needs

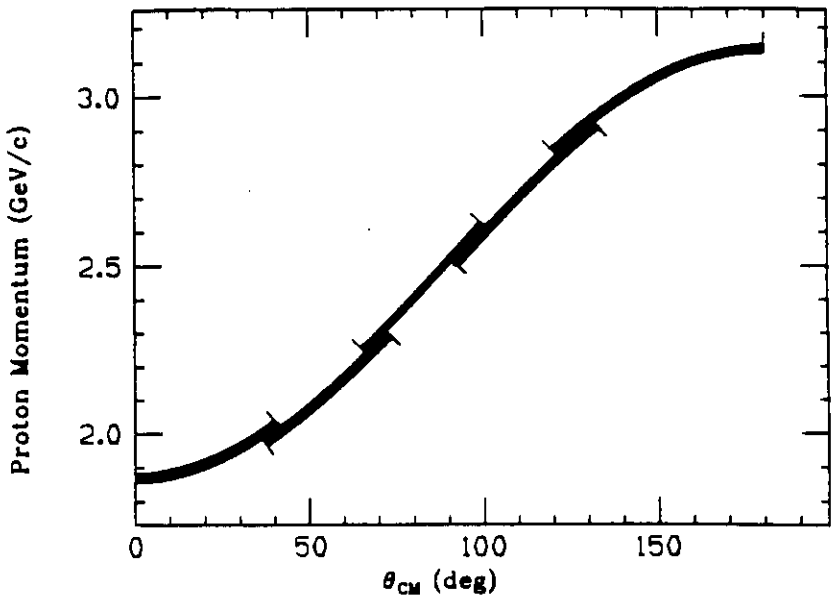

Figure 8. The acceptance of the HMS spectrometer in delta cm decay angle and proton momentum for the HMS lab. angular settings shown in Figure 7. The finite acceptance of the SOS will significantly broaden and overlap the acceptances shown in the figure.

to be determined - see discussion above). This is seen as follows. The expression of the coefficients in eq. 4 above in terms of multipoles is given in the Appendix. For simplicity, in eq. A1 we retain only M_{1+} and E_{1+}, and we neglect multipoles of order $|E_{1+}|^2$. Under these conditions the only remaining coefficients in eq. 4 are A and C, which may be written

$$A = A_0 + A_2 cos^2(\theta) \quad \text{with,} \tag{6a}$$

$$A_0 = \tfrac{5}{2}|M_{1+}|^2 - 3Re(M_{1+}E^*_{1+}) \tag{6b}$$

$$A_2 = -\tfrac{3}{2}|M_{1+}|^2 + 9Re(M_{1+}E^*_{1+}) \tag{6c}$$

$$C = C_0 = -\tfrac{3}{2}|M_{1+}|^2 - 3Re(M_{1+}E^*_{1+}) \tag{6d}$$

The factor of 9 in eq. 6c results in a very large angular sensitivity to $Re(M_{1+}E^*_{1+})$.

Differential cross section were calculated at $Q^2 = 4\ GeV^2/c^2$ assuming the ratio E/M = 0, 0.1 and 0.2. The calculations use the full expression, without any assumptions about the magnitude of E/M, but with the assumptions $S_{1+} = 0$, and that the phases of E_{1+} and M_{1+} are equal. The calculations also include the non-resonant Born amplitudes up to a partial wave L = 5. The multipole amplitudes for all cases were normalized to yield the same angle integrated resonance cross section $\sigma(W_R) = 3.3\mu b$ as estimated from St-91a,b. These amplitudes are as shown in Table I.

Angular distributions in θ for three values of fixed ϕ are shown in Figure 9a-c respectively.

One observes that there is a great deal of sensitivity to the ratio E/M over much of the $(cos(\theta) - \phi)$ kinematic plane, whereas the lack of sensitivity at other regions will serve as an important constraint on the overall analysis. Also shown in Figure 9 is the non-resonant Born contribution, which is seen to be rather small. Other backgrounds, such as tails of higher resonances, will also contribute. One of the goals of our theoretical effort will be to characterize this background. The relative contribution of the background terms will be further reduced by selecting only $l = 1$ partial waves in the analysis. An important handle on the non-resonant contributions will be obtained by analysis of the data away from the central resonance energy. Figure 10 shows the angular distribution in θ for the same values of ϕ as in Figure 9, but off-resonance with baryon mass $W = W_R + 100MeV = 1323MeV$. Here the non-resonant terms are comparable to the resonant terms giving rise to strong interference effects.

Asymmetries inherent in the cross sections of Figures 9 and 10 are very sensitive, to E/M. For example, Figure 11 shows the ϕ dependence of the asymmetry

$$\Sigma(\phi)_{(90-0)} \equiv \frac{\sigma(\theta = 90°) - \sigma(\theta = 0°)}{\sigma(\theta = 0°)} \tag{7a}$$

at $W = W_R$ and $W = W_R + 100\ MeV$.

Figure 12 show the asymmetries

$$\Sigma(\theta)_{(\theta-0)} \equiv \frac{\sigma(\theta) - \sigma(\theta = 0°)}{\sigma(\theta = 0°)}. \tag{7b}$$

for three fixed values of ϕ, on resonance at $W = 1232\ MeV$ and off-resonance at $W = 1332\ MeV$.

One sees that the asymmetries are extremely sensitive to the assumed values of E/M. Note that in Figures 11 and 12 off resonance at $W = 1323\ MeV$ the interference between resonant and non resonant terms are now very important, leading to remarkable effects in the relative signs of the asymmetries as a function $cos(\theta)$ depending on the fixed value of ϕ.

VI. Statistical Accuracy of the Data

Estimates for the expected statistical accuracy of the data were carried out on the basis of the assumptions which are given in Table I.

The total number of events expected over a 10 day collection period for $W = 1232 \pm 50MeV$ over 4π cm delta decay is about $1/2 \times 10^6$, with lesser amounts as we go off resonance. In Figures 9 through 12 are plotted the expected statistical accuracy of the

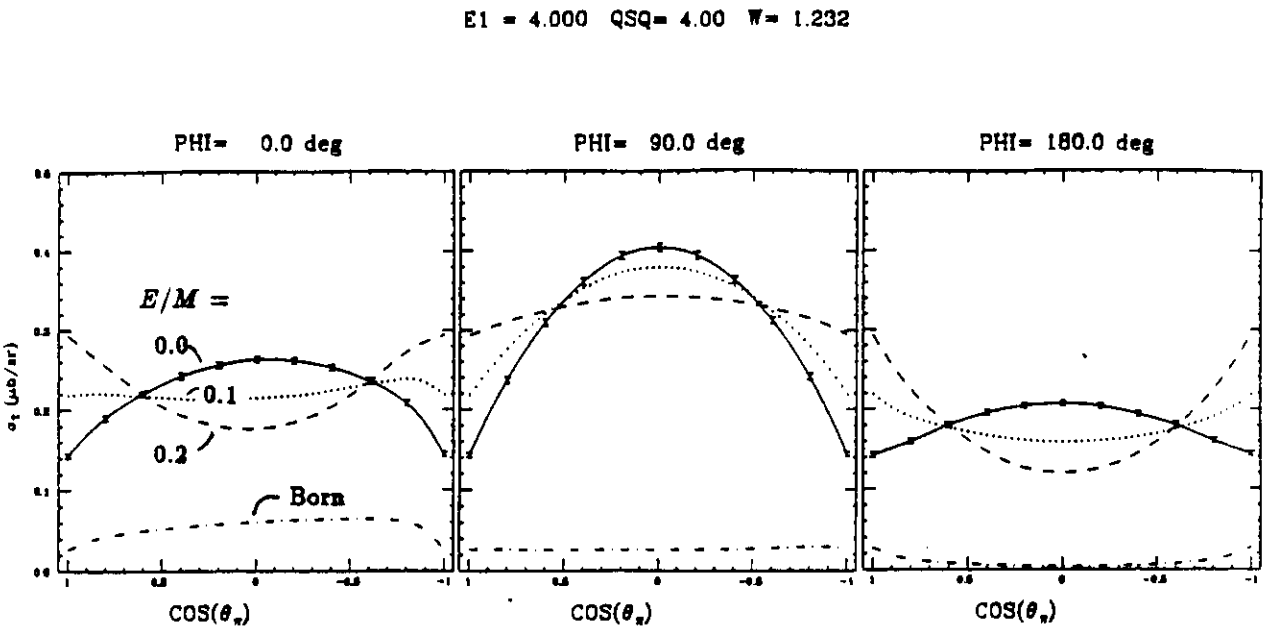

Figure 9. Calculated differential cross sections vs θ_{cm} of the detected proton at fixed values of ϕ_{cm} for the reaction $p(e,e'p)\pi^o$ at $Q^2 = 4\ GeV^2/c^2$, at $W = W_R = 1232MeV$, including Born amplitudes, assuming a total resonance inclusive virtual cross section $\sigma = 3.3\mu b$. The three curves in each figure correspond to $E/M = 0.0$, 0.1 and 0.2 respectively. The dotted points are the calculated non-resonant Born terms obtained by setting the resonant amplitudes to zero. The points with error bars are the expected statistics of the proposed experiments, under the data binning conditions discussed in the text. There will actually be a total of 9 such distributions in the experiment.

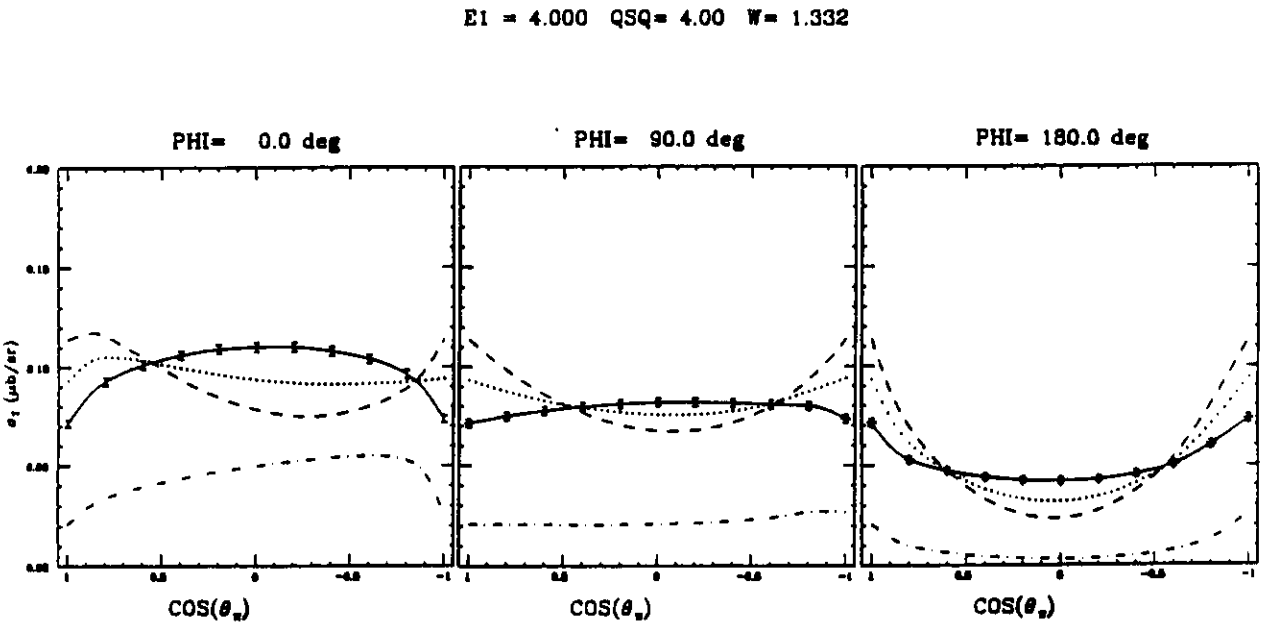

Figure 10. Same as in Figure 9, but at $W = W_R + 100MeV$.

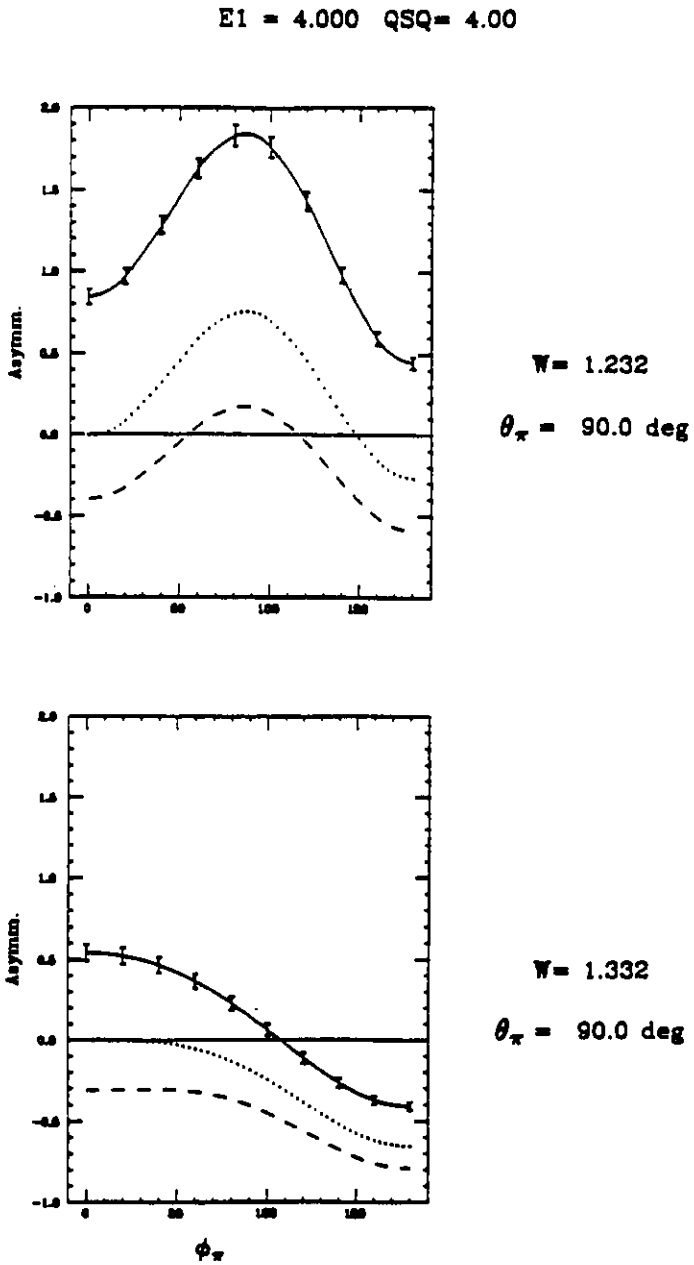

Figure 11. The calculated ϕ dependence of the asymmetry $\Sigma(\phi)_{(90-0)}$ at $W = 1232$ and $1323\ MeV$. The curves have the same meaning as in Figure 9.

differential cross sections. Each point represents the data binned over the interval $\Delta cos\theta = 0.2, \Delta\phi = 40°$. The statistical relative standard deviation for one data point is typically 1/2 % on resonance and about 1% for the adjacent off resonance intervals. There will be about 100 such data points over 4π for each W interval. The statistical uncertainties on the asymmetries are also very small, typically between 1 and 2%.

VII. Systematic Errors

A very important control for this experiment is that at several kinematic settings of the proton detector we simultaneously collect data on the elastic channel $p(e, e'p)$. Since

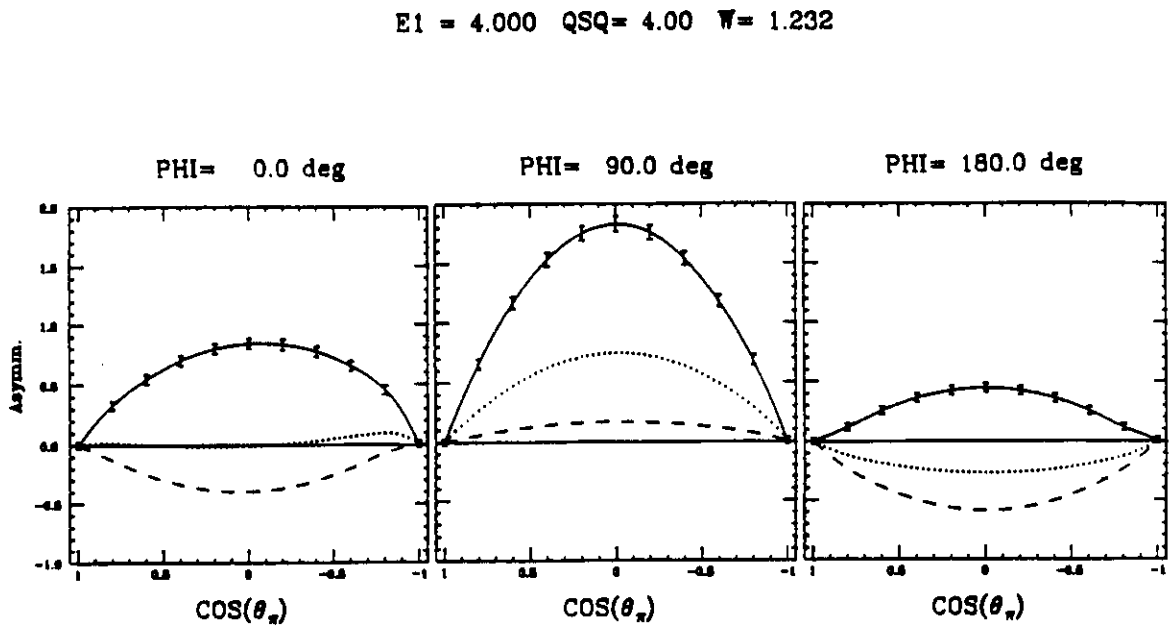

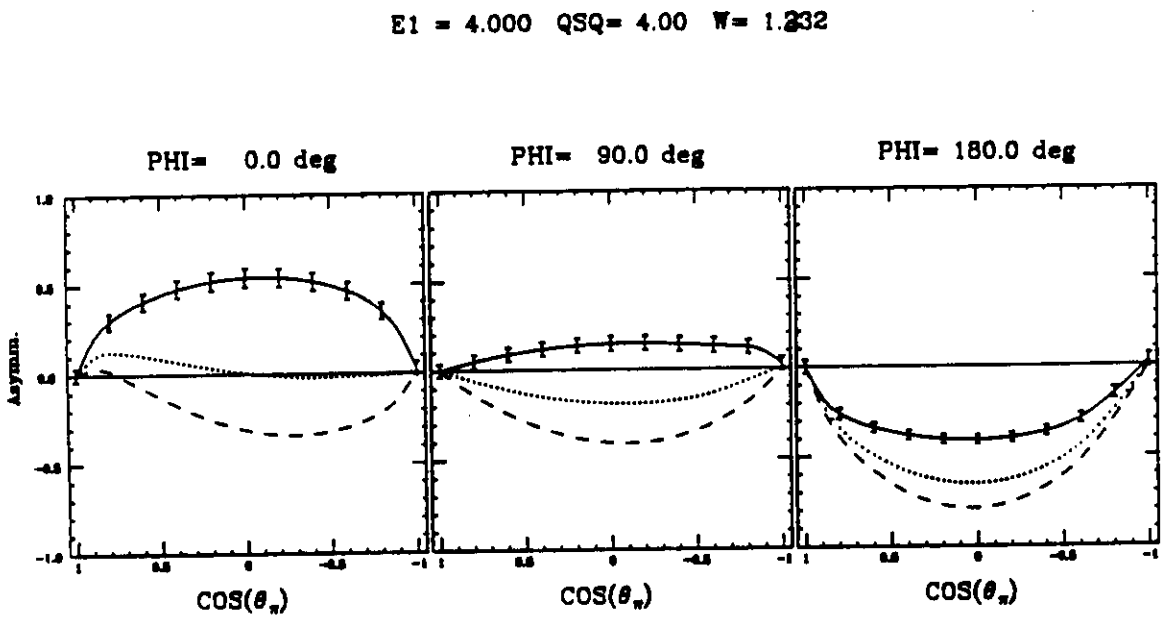

Figure 12. The asymmetries $\Sigma(\theta)_{(\theta-0)}$ for different fixed values of ϕ, on resonance at $W = 1232\ MeV$ and at $W = 1332\ MeV$. The curves have the same meaning as in Figure 9.

- Cross section $\sigma(W_R) = 3.3\mu b$

- Amplitudes

$E/M = 0.0 \qquad M_{1+} = -.362\ \mu b^{1/2} \qquad E_{1+} = 0\ \mu b^{1/2}$

$E/M = 0.1 \qquad M_{1+} = -.357\ \mu b^{1/2} \qquad E_{1+} = -.036\ \mu b^{1/2}$

$E/M = 0.2 \qquad M_{1+} = -.343\ \mu b^{1/2} \qquad E_{1+} = -.069\ \mu b^{1/2}$

- Electron arm (SOS)

$\theta_e = 48^\circ \quad P_e = 1.53 GeV/c$

Solid angle of acceptance $\Omega = 5\ msr$

ΔW selected $= 100\ MeV$

- Proton arm (HMS)

$\theta_q = 21^\circ \quad P_{max} = 3.1 GeV/c \quad P_{min} = 1.8 GeV/c$

$\Delta x\ (out - of - plane) = 165\ mrad$

$\Delta y\ (in - plane) = 50\ mrad$

$\Delta P/P = 0.20\ (0.10)$

Total number of angle and momentum settings = 8

- Time of data collection = 10 days (240 hrs)

- Luminosity $1 \times 10^{38}\ cm^{-2}s^{-1}$ $(I = 100\mu A,\ X_{target} = 4cm)$

- Total number of events over $\Omega = 4\pi$ (within $W = 1232 \pm 50 MeV$) $\sim 1/2 \times 10^6$

Table I. The kinematic conditions and acceptances used in estimating the statistics which would be expected for the experiment.

these cross sections are well known at the Q^2 of this experiment, this will serve as a very accurate normalization for our data. That is, it will pin down the product $N_e X_{target} \Omega_e \Omega_p$. Furthermore, the electron spectrometer (SOS) will always be run at the same angle and momentum settings so that by accumulating pre-scaled singles we will automatically get an accurate relative normalization for the runs involving different proton spectrometer (HMS) settings, which will be extremely useful when the data are combined. Thus, in a sense the experiment will be self normalizing. In obtaining the asymmetries such as those in eqs. 7 the normalization factors cancel so that the systematic uncertainties would be even smaller.

References:

(Ar-86) R.G. Arnold et al., Phys. Rev. Lett., **57**, (1986) 174.
(Am-92) T.A. Armstrong et al., Phys. Rev. Lett., **70** (1993) 1212.
(Bl-71) E. Bloom and F.J. Gilman, Phys. rev., **D4** (1971) 2901.
(Br-84) F. W. Brasse et al., Z. Phys. **C22** (1984) 33.
Nuc. Phys.**B139**(1978) 37.
(Br-89) S.J. Brodsky, Lectures at the 27th International School of Subnuclear Physics, Ettore Majorana Center for Scientific Culture, Erice (1989),SLAC-PUB-5116, and references therein. and P.Stoler,eds.,World Scientific, Singapore (1989), p122.
(Bu-91) V. Burkert, private communication.
(Bu-92) V. Burkert, private communication.
(Ca-88) C.E. Carlson and J.L. Poor, Phys. Rev. **D38**, (1988) 2758 .
(Ca-92) C.E. Carlson and N.C. Mukhopadhyay, too be published
(Ch-84) V.L. Chernyak and A.R. Zhitnitsky, Phys. Rep. **112** (1984) 73
(Da-90) R.M. Davidson and N.C. Mukhopadhyay, Phys. Rev. **D42**, 20 (1990)
(Da-91) R.M. Davidson, N.C. Mukhopadhyay, and R. Whittman, Phys. Rev. **D43**, 71 (1991)
(Do-78) A. Donnachie, G. Shaw, and D.H. Lyth in 'Electromagnetic Interactions of Hadrons', A. Donnachie and G. Shaw, eds., Plenum, New York (1978)
(Dz-88) Z. Dziembowski, Phys. Rev., **D37** (1988) 778.
(Fo-83) F. Foster and G. Hughes, Rep. Prog. Phys. **46** (1983) 1445.
(Ga-86) M. Gari and N.G. Stephanis, Phys. Lett **B175**, (1986) 462
M. Gari and W. Krupelmann, Phys. Lett. **B173**(1986)10 .
(Ha-79) R. Haiden, DESY rep. F71-79/03
(Is-89) N. Isgur and C.H. Llewellyn-Smith, Phys. Lett. **217B**,(1989)535.
(Ji-87) C-R. Ji, A. Sill, and R. Lombard-Nelson, Phys. Rev. **D36**,(1987) 165
(Ki-87) I.D. King and C.T. Sachrajda, Nucl. Phys. **B279** (1987) 785.
(Li-92) H-N. Li, SUNY-Stony Brook report ITP-SB-92-25
(Ra-91) A.V. Radyushkin, Nucl. Phys. **A527**, 53 (1991).
(St-91a) P. Stoler, Phys. Rev. Lett., **66** (1991) 1003 .
(St-91b) P. Stoler, Phys. Rev. **D44** (1991) 73.
(St-93) P. Stoler, Physics Reports, to be published.
(Wa-90) G.A. Warren and C.E. Carlson, Phys. Rev. **D42** (1990) 3020.

Appendix. Relationship Between Multipoles and Measured Data

With unpolarised beam and target the double differential cross section for electrons and pions may be written

$$\frac{d\sigma}{d\Omega_e dE d\Omega_\pi} = \Gamma \frac{d\sigma}{d\Omega_\pi}. \tag{5}$$

where $d\sigma/d\Omega_\pi$, the virtual photon cross section for pions emitted at angles (θ, ϕ) relative to the direction of the virtual photon, may be expressed as

$$\frac{d\sigma}{d\Omega_\pi} = F\{A(\theta) + \epsilon B(\theta) + \epsilon C(\theta) cos(2\phi) sin^2\theta + \sqrt{\epsilon(\epsilon+1)} D(\theta) cos\phi sin\theta.\} \tag{6}$$

In eq. 5 Γ is the virtual photon flux factor

$$\Gamma = \frac{\alpha K}{2\pi^2 Q^2} \frac{E'}{E} \frac{1}{1-\epsilon},$$

$$F \equiv \frac{|\vec{p}_\pi| W}{M K},$$

and K is the equivalent real photon energy

$$K = \frac{W^2 - M_N^2}{2M_N}.$$

Defining $\bar{A}_i \equiv A_i + \epsilon B_i$, the multipole decomposition of the coefficients up to a maximum $l = 1$ are (see Do-78):

$$\begin{aligned}
\bar{A}_0 = \{&|E_{0+}|^2 + |M_{1-}|^2 + \tfrac{3}{2}|M_{1+}|^2 + \tfrac{9}{2}|E_{1+}|^2 - 3\,\mathrm{Re}(M_{1+}E_{1+}^*) \\
&+ \mathrm{Re}[(3E_{1+} + M_{1+})M_{1-}^*] \\
&+ \epsilon(|k^2|/|\mathbf{k}|^2)[|S_{0+}|^2 + |S_{1-}|^2 + 4|S_{1+}|^2 - 4\,\mathrm{Re}(S_{1+}S_{1-}^*)]\} \\
\bar{A}_1 = \{&2\,\mathrm{Re}[E_{0+}(3E_{1+} + M_{1+})^*] + \epsilon(|k^2|/|\mathbf{k}|^2) 2\,\mathrm{Re}[S_{0+}(4S_{1+} + S_{1-})^*]\} \\
\bar{A}_2 = \{&-\tfrac{3}{2}|M_{1+}|^2 + \tfrac{9}{2}|E_{1+}|^2 + 9\,\mathrm{Re}(M_{1+}E_{1+}^*) - 3\,\mathrm{Re}[(3E_{1+} + M_{1+})M_{1-}^*] \\
&+ \epsilon(|k^2|/|\mathbf{k}|^2)[12|S_{1+}|^2 + 12\,\mathrm{Re}(S_{1+}S_{1-}^*)]\} \\
C_0 = \{&-\tfrac{3}{2}|M_{1+}|^2 + \tfrac{9}{2}|E_{1+}|^2 - 3\,\mathrm{Re}(M_{1+}E_{1+}^*) + 3\,\mathrm{Re}[(E_{1+} - M_{1+})M_{1-}^*]\} \\
D_0 = -\{&|k^2|/|\mathbf{k}|^2\}^{1/2}\,\mathrm{Re}[S_{0+}(3E_{1+} - M_{1+} + M_{1-})^* - E_{0+}(2S_{1+} - S_{1-})^*] \\
D_1 = -6\{&|k^2|/|\mathbf{k}|^2\}^{1/2}\,\mathrm{Re}[S_{1+}(E_{1+} - M_{1+} + M_{1-})^* + S_{1-}E_{1+}^*]
\end{aligned}$$

By retaining only M_{l+} and E_{l+}, and neglecting terms in $|E_{l+}|^2$ yields eqs. 6 in the text.